DOI: 10.1002/ange.201300183

Drug Delivery

NIR-Triggered Anticancer Drug Delivery by Upconverting Nanoparticles with Integrated Azobenzene-Modified Mesoporous Silica**

Jianan Liu, Wenbo Bu, Limin Pan, and Jianlin Shi**

Cancer is one of the most common causes of death in the world, and chemotherapy remains to be one of the most frequent treatments for many cancers. However, its success has been greatly limited because of systemic toxicity due to the toxic effects by the nonspecific distribution of anti-cancer drugs. The drug delivery systems with the features of sustained drug release have attracted much attention owing to their enhanced therapeutic efficacy and reduced side effect.[1] For example, mesoporous silica nanoparticles (MSNs) with interesting properties, such as thermal and photostability, tunable sizes, high loading capacity, and the ease of functionalization according to currently available results, have made the MSNs one of the most promising carriers for drug delivery.[2] Although MSNs-based drug delivery systems have been proven effective, however, the use of cytotoxic drugs that are only released in the target area is much more preferred in clinical application. One way to prevent any premature release of anticancer drugs before they reach the target cells is to develop stimuli-responsive systems with controlled release features. Over the past decade, researches on MSNs-based light-controlled drug delivery systems have been carried out extensively because light as an external stimulus offers controllable drug release both spatially and temporally and thus exhibits great potentials for further biomedical applications.[3] However, most of them have achieved limited success in applications in vitro and in vivo mainly because of the easy damages to both biological samples and living tissues by UV light used to excite the photosensitizer and extremely quick attenuation of UV light in tissues. To tackle this issue, it is highly desirable to develop NIR remote-controllable MSNs-based system which can be used both in vitro and in vivo, which, however, has not been well addressed and remains a great challenge.

Compared to UV light, near-infrared (NIR) light is much less damaging to biological specimens and living tissues involved and has remarkably deeper tissue penetration.[4] For example, Parak and co-workers reported that polyelectrolyte multilayer capsules loaded with cargo and plasmonic (Au or Ag) NPs can be used to release the cargo by NIR-photothermal heating.[5] The cargo can be easily released with high efficiency under NIR exposure in one second. However, the size of these capsules can be as large as several microns, which will inevitably suffer from phagocytosis by reticuloendothelial systems (RES) when these systems are intravenously injected. Recently, upconverting nanoparticles (UCNPs) have emerged as an appealing candidate for the application of NIR light.[6] Because of the unique ladder-like energy level structures of lanthanide ions (such as Tm^{3+}, Er^{3+}, and Ho^{3+}), UCNPs are able to absorb NIR light and convert it into high-energy photons in a very broad range from the UV to the NIR region. Such a unique and fascinating photoluminescence property enables UCNPs to function as a NIR-induced mediator by coating caged compounds on the nanoparticle surface,[7] and as a NIR-controlled photoswitch for reversible ring-closing and ring-opening transformation of a dithienylethene compound.[8] Very recently, Branda and co-workers successfully used the NIR laser to dissociate block copolymer micelles by encapsulating UCNPs inside micelles.[9] Since the copolymer micelles will inevitably suffer from self-degradation in biological environment, a combination between UCNPs and micelles may find few opportunities in practical bio-applications for remote-controlled drug delivery using a NIR laser in vitro and in vivo. In more recent studies, our group successfully demonstrated UCNP/methylene blue-based photodynamic therapy (PDT) through controlled singlet oxygen release triggered by NIR light.[10] However, in spite of all the above efforts, reports on the direct NIR-light-controlled anticancer drug release for cancer therapy from a UCNPs-containing structure has not been found in the literature to date, which remains a great challenge in light-controlled drug delivery studies.

Herein, we report a novel and general strategy for NIR light-triggered anticancer drug release based on a mesoporous silica-coated UCNPs structure, designated as UCNP@$mSiO_2$. Figure 1a shows the synthetic procedure for UCNP@$mSiO_2$. The strategy consists of preparing $NaYF_4$: TmYb@$NaYF_4$ core–shell nanoparticles and subsequently coating the Tm-doped core–shell UCNPs with mesoporous silica. After

[*] J. N. Liu, Prof. W. B. Bu, L. M. Pan, Prof. J. L. Shi
State Key Laboratory of High Performance Ceramics and Superfine Microstructure
Shanghai Institute of Ceramics, Chinese Academy of Sciences
1295 Ding-Xi Road, Shanghai 200050 (China)
E-mail: wbbu@mail.sic.ac.cn
jlshi@sunm.shcnc.ac.cn

[**] This work was financially supported by the National Natural Science Foundation of China Research (grant numbers 50823007, 50972154, 51132009, 51072212, and 21172043), the Shanghai Rising-Star Program (grant number 12QH1402500), the Nano special program of the Science and Technology Commission of Shanghai (grant number 11nm0505000), the Development Foundation for Talents of Shanghai (grant number2012035), the National Basic Research Program of China (973 Program, grant number 2011CB707905).

Supporting information for this article is available on the WWW under http://dx.doi.org/10.1002/anie.201300183.

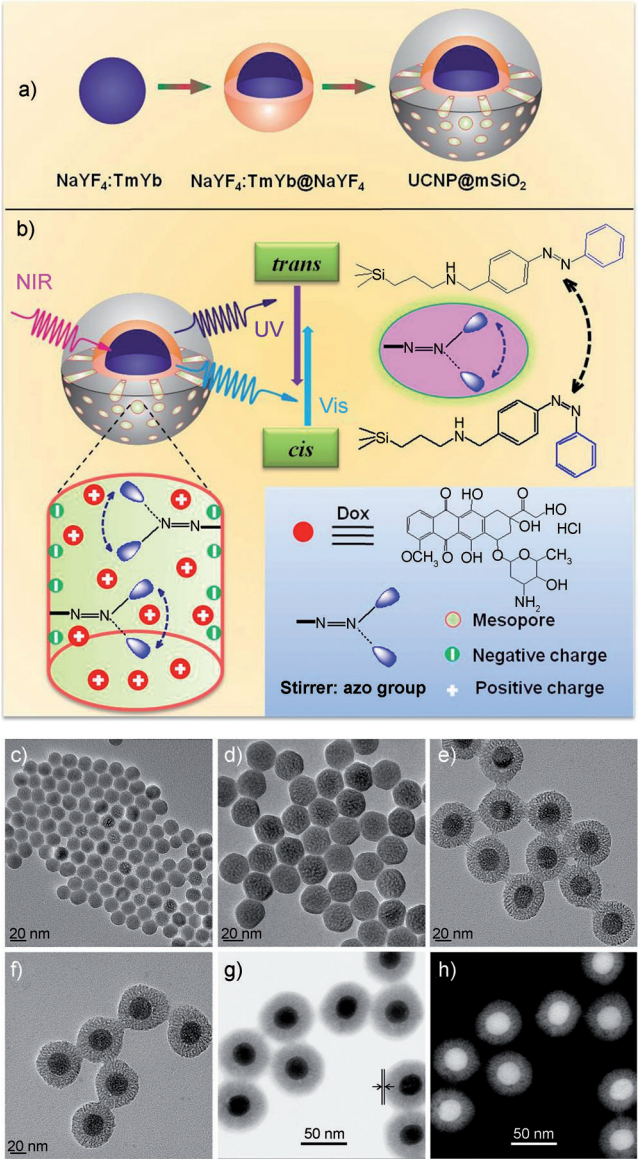

Figure 1. a) Synthetic procedure for upconverting nanoparticles coated with a mesoporous silica outer layer. b) NIR light-triggered Dox release by making use of the upconversion property of UCNPs and *trans–cis* photoisomerization of azo molecules grafted in the mesopore network of a mesoporous silica layer. TEM images of c) $NaYF_4$:Tm, Yb, d) $NaYF_4$:Tm, Yb@$NaYF_4$, e) $NaYF_4$:Tm, Yb@$NaYF_4$@$mSiO_2$, and f) $NaYF_4$:Tm, Yb@$NaYF_4$@$mSiO_2$-azo. g) Bright-field and h) dark-field STEM image of TAT-modified $NaYF_4$:Tm, Yb@$NaYF_4$@$mSiO_2$-azo.

installing "photomechanical" azobenzene groups (azo) into the mesopores of silica that act as "stirrer" in the mesoporous silica, the TAT peptide was conjugated on the surface of the NPs to enhance the cellular uptake.[11] The above materials were called UCNP@$mSiO_2$-azo. Finally, the anticancer drug doxorubicin (Dox) was loaded into the mesopores (Dox-UCNP@$mSiO_2$-azo). Dox (zeta potential: +2.2 mV) can strongly attach to silica (zeta potential: −40.6 mV) through formation of strong hydrogen bonds and charge interactions with the surface silanol groups,[12] which resulted in a minimal Dox release in aqueous environments. While the *trans* isomer of the azo molecules will transform into the *cis* isomer under UV light irradiation, and in contrast the *cis* isomer will form the *trans* isomer under irradiation of visible light (Figure S1 in the Supporting Information). Upon absorption of NIR light (980 nm), the nanoparticles emit photons in the UV/Vis region, which can be absorbed immediately by the photo-responsive azo molecules in the pore network of the mesoporous silica layer (Figure 2a). The reversible photo-isomerization by simultaneous UV and visible light emitted by the UCNPs creates a continuous rotation–inversion movement. The back and forth wagging motion of the azo molecules will act as a molecular impeller that propels the release of Dox. As a result, the Dox loaded in the mesopores

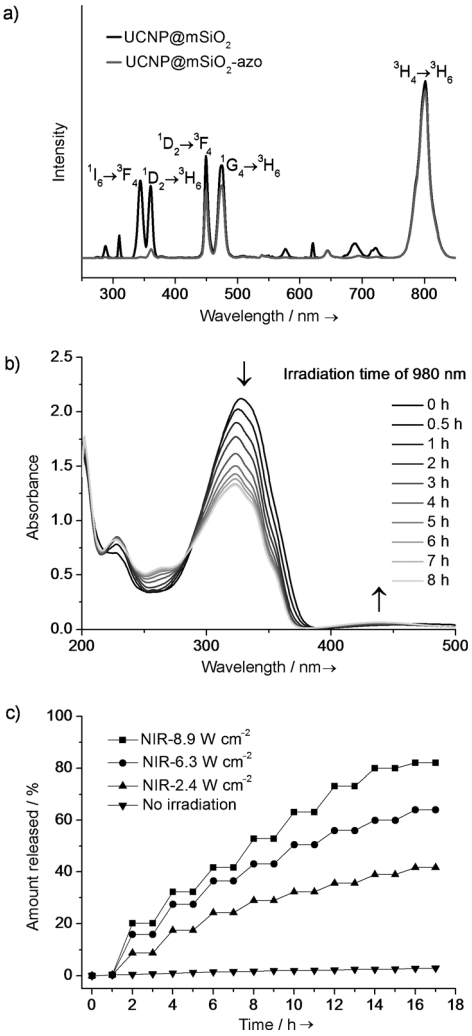

Figure 2. a) Emission spectra of UCNP@$mSiO_2$ and UCNP@$mSiO_2$-azo from UV to NIR light at the same UCNP concentration upon diode laser light exposure at 980 nm. The UV and visible light have been mostly and partially absorbed whereas NIR light (800 nm) from UCNPs retained the original luminescent intensity even after the modification by azo molecules in the mesopores, demonstrating the high efficient use of the upconverted UV and visible light in *trans--cis* photoisomerization of azo molecules and the 800 nm NIR light for additional luminescent imaging. b) UV/Vis absorption spectra of UCNP@$mSiO_2$-azo before and after irradiation with 980 nm light (8.9 $W cm^{-2}$) for 0.5 to 8 h. c) Drug release in PBS under NIR light irradiation and dark conditions, alternatively. Every duration of NIR irradiations is 1 h.

can be released in a controllable fashion, as illustrated in Figure 1b. Multifunctional applications can be achieved by upconversion luminescence from the UCNPs. On one hand, upconverted UV and visible light can excite the azo group for controlled drug release; on the other hand, synchronously emitted upconverted NIR light is very suitable for in vivo luminescent imaging of whole-body animals with enhanced penetration depth.[13]

As a starting point of our study, the core–shell $NaYF_4$:TmYb nanoparticles (core = $NaYF_4$: 0.5 mol% Tm^{3+} 20 mol% Yb^{3+}; shell = $NaYF_4$) were synthesized using reported methods.[14] Transmission electron microscopy (TEM) images of the UCNPs demonstrate their nearly monodisperse particle size of about 17 and 28 nm for core and core–shell nanoparticles, respectively (Figure 1c,d). The core–shell UCNPs are highly crystalline and hexagonal in phase, as confirmed by powder X-ray diffraction (Figure S2), and exhibit enhanced fluorescence emission compared to core-only nanoparticles (Figure S3). Afterwards, we succeeded in coating the UCNPs with the mesoporous silica outer layers by first removing the oleate ligand from the surface of oleate-capped UCNPs through HCl treatment[15] and then adding this oleate-free UCNPs to aqueous media containing triethanolamine (TEA), cetyltrimethylammonium chloride (CTAC), and tetraethylorthosilicate (TEOS) to induce the self-assembly of the mesoporous silica outer layers on the UCNPs.[16] The size of the resulting upconversion nanoparticles coated with mesoporous silica is around 54 nm, as measured by TEM (Figure 1e). After removal of CTAC and centrifugation, the resulting UCNP@$mSiO_2$ was modified with *N*-(3-triethoxysilyl)-propyl-4-phenylazobenzamide inside the mesopores. It was calculated from UV/Vis spectra that the above materials contain about 1.6 wt% of the azobenzene derivatives. Finally, the TAT peptide was linked on the outer surface to enhance cellular uptake, and this modified sample was loaded with 5 wt% of doxorubicin (Dox). As shown in Figure 1g by scanning transmission electron microscopy (STEM), the TAT coating had a relatively uniform thickness of about 4 nm. This result is in reasonable agreement with the value estimated from dynamic light scanning (Figure S7).

Figure 2a shows the emission spectra of UCNP@$mSiO_2$ and UCNP@$mSiO_2$-azo at the same UCNP concentration upon excitation at 980 nm. As compared to UCNP@$mSiO_2$, the emission intensity of UV and visible light from the UCNP@$mSiO_2$-azo is remarkably depressed, indicating that the UV and visible photons delivered by the UCNPs have been greatly and partially absorbed by azo moieties in the mesoporous silica shell, respectively. The absorption spectra of UCNP@$mSiO_2$-azo before and after exposure to NIR light for varied time intervals were also shown in Figure 2b, which illustrates how the absorption spectrum of azo molecules partially overlaps ($\lambda_1 = 330$ nm, $\lambda_2 = 440$ nm) with the emission spectrum of UCNPs ($\lambda_1 = 350$ nm, $\lambda_2 = 450$ nm). With the increase of NIR irradiation duration, the absorbance of the maximal absorption band of the azo moiety at 330 nm decreases apparently, which has a spectral profile the same as those recorded when UCNP@$mSiO_2$-azo are exposed directly to UV light (Figure S9). Exposure of azo-modified mesoporous silica nanoparticles to 980 nm NIR laser light resulted in no observable change in the UV/Vis absorption spectrum even after 24 h of irradiation (Figure S10), demonstrating that the azo molecule is not susceptible to NIR light in the absence of the UCNPs. These results confirm that it is the UV and visible light from UCNPs that causes the *trans–cis* photoisomerization of the azo molecules in the mesoporous silica layer.

To investigate the photoinduced controlled release property of Dox-UCNP@$mSiO_2$-azo, a solution of Dox-UCNP@$mSiO_2$-azo was then exposed to alternating periods of NIR light irradiation at 2.4–8.9 $W cm^{-2}$ (Supporting Information, Section 1.17). The precise control of drug release was demonstrated by monitoring the concentration of the released anticancer drug after alternating periods of exposure to NIR light and dark conditions as shown in Figure 2c. The Dox release amount controlled by NIR light reached 40 wt% in 16 h under intermittent NIR exposures (2.4 $W cm^{-2}$), and reached a maximum of 80 wt% in 16 h of 980 nm laser light irradiation of 8.9 $W cm^{-2}$, indicating that the release rate increased at the enhanced external NIR intensity. A control experiment without NIR irradiation was also carried out. Less than 5 wt% of Dox was leached into the aqueous solution in 17 h of placement. The distinctive "stepped" profile of the drug release shows that the drug release can only be triggered by NIR exposure and the amount of the released drug is highly dependent on the duration and intensity of NIR exposure, thus realizing "NIR light-regulated precise drug release".

Based on the successful operation of the azo impeller in water, controlled drug release studies were carried out by incubating with HeLa cells to validate the feasibility of using this system in vitro. After 3 h of incubation in the dark with Dox-UCNP@$mSiO_2$-azo, the cells were exposed to three different 980 nm excitation intensities (2.4, 6.3, and 8.9 $W cm^{-2}$) with exposure durations ranging from 0 to 20 minutes. After a further incubation for 1 h to ensure the sufficient diffusion of the released Dox, the cells were examined by confocal microscopy. As can be seen from Figure 3a, no free Dox could be detected in the cell without NIR light exposure. In sharp contrast, under the identical experimental conditions but being exposed to NIR light (2.4 $W cm^{-2}$, 5 minutes), free Dox was detected in the cytoplasm. Clearly, a longer exposure duration (10, 15, and 20 minutes) resulted in stronger Dox fluorescence. The increasing red light intensity over time indicates a continuous Dox release which resulted from the azo-impeller operation. Stronger Dox fluorescence was observed in the cell nucleus after NIR excitation (8.9 $W cm^{-2}$) for 20 minutes (Figure S20). These results verify that the amount of released Dox is directly related to the total number of photons absorbed from the emitting UCNPs. Additionally, we also carried out flow cytometry experiments to quantify the cellular uptake of Dox by HeLa cell nuclei. As shown in Figure 3b, with the increase of the exposure time of NIR light, more Dox can be found in the cell nuclei. These results confirmed that the Dox released in cytoplasm can migrate into nucleoplasm to kill the cancer cells. We also carried out control experiments where NPs without TAT inside cells were

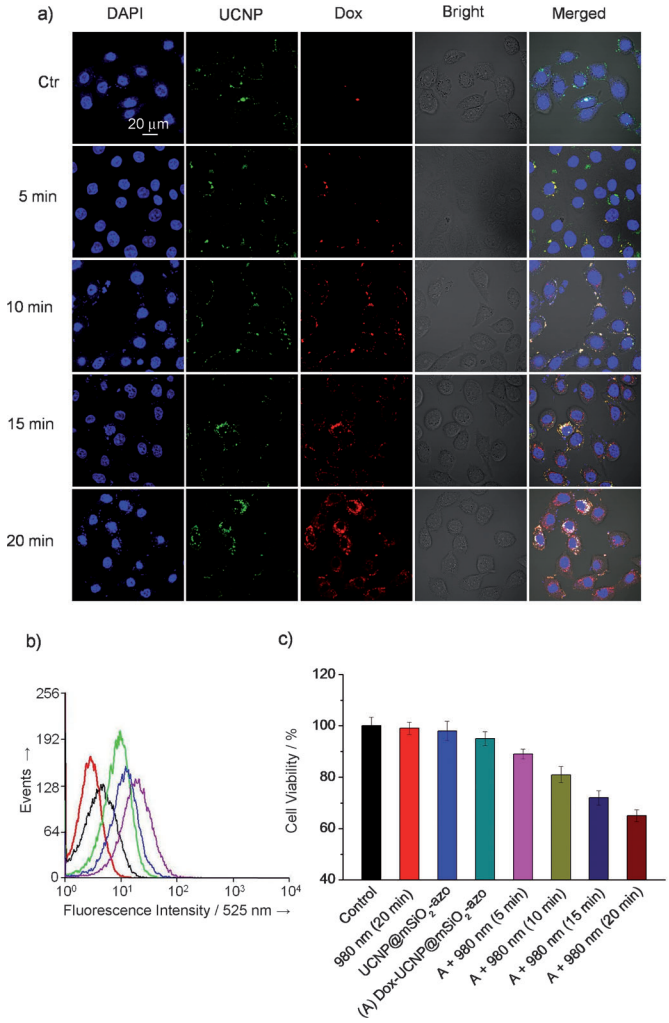

Figure 3. a) CLSM observations of the photocontrolled Dox release in HeLa cells. Dox-UCNP@mSiO$_2$-azo was pre-incubated with the cells for 3 h in the dark. After the incubation, the cells were washed twice with medium and then irradiated with a 980 nm continuous-wave NIR laser for 5 to 20 minutes. Then, the cells were examined with confocal microscopy. For each panel, the images from left to right show cell nuclei stained by DAPI (blue; DAPI = 4',6-diamidino-2-phenylindole), UCNP fluorescence in cells (green), Dox fluorescence in cells (red), bright field, and overlays of the four images. All images share the same scale bar (20 μm). b) After further incubation in the dark for 24 h, flow cytometry histograms were performed under excitation of 488 nm laser light, which show the Dox fluorescence intensity in HeLa cell nuclei separated from the whole cell. The red lines represent the results of negative control samples where no NIR light is present. The black, green, blue and purple lines show the results of samples treated with NIR light exposure for 5, 10, 15, and 20 minutes. The cell counts were 20000. c) Inhibition of HeLa cell growth in the presence of excitation at 980 nm (20 minutes), UCNP@mSiO$_2$-azo, and Dox-UCNP@mSiO$_2$-azo without or with NIR light exposures for varied durations/dosages after 24 h of incubation. The concentration of the MSN materials was 1 mg mL^{-1}, and the NIR light exposure intensity was 2.4 W cm^{-2}.

photoexcited by NIR (Figures S24 and S25). The results showed that enhanced intracellular delivery of TAT-NPs resulted in significantly lower cell viability, indicating that more Dox molecule are released compared with NPs without TAT under identical NIR exposure. As a result, the combination between the TAT and NIR-triggered drug release clearly makes a very efficient NIR-controlled release system.

The in vitro cytotoxicity of Dox-UCNP@mSiO$_2$-azo under exposure to 980 nm light was evaluated by the MTT assay. We incubated HeLa cells in the culture medium with Dox-UCNP@mSiO$_2$-azo under NIR excitation, and with UCNP@mSiO$_2$-azo, NIR excitation, and Dox-UCNP@mSiO$_2$-azo treatments as the controls. After 3 h of incubation, the NPs were removed and the cells were further incubated for 24 h in the dark. Treatments with UCNP@mSiO$_2$-azo loaded with and without Dox did not result in a significant decrease in the cell viability, indicating the negligible delivery of Dox into the HeLa cells, because of the absence of an impelling effect of the azo molecules in the dark. In contrast, Dox-UCNP@mSiO$_2$-azo upon irradiation at 980 nm showed a significantly enhanced cytotoxicity to the cancer cells, which could be explained by the controlled drug release and significant accumulation of Dox inside the cells (Figure 3c). This finding is in line with the confocal laser scanning microscopy (CLSM) results that the impeller operation can be regulated by the light intensity and time duration, thus the amount of the released Dox can be controlled. In vitro controlled drug delivery experiments with other four cell lines: two normal cells (L929 fibroblast cells, human embryonic kidney 293T cells) and two cancer cells (U87 MG human glioblastoma cells, murine 4T1 breast cancer cells) were also performed (Figure S26–S28). Similar results with HeLa cells were observed, further confirming the potential of the NIR-triggered drug delivery system.

In summary, a new paradigm for the precise in vitro control of drug dosing using NIR light has been demonstrated. By coating NaYF$_4$: TmYb UCNPs with azo-modified mesoporous silica and using 980 nm light, the amount of the released anticancer drug can be well controlled by varying the intensity and/or time duration of NIR light irradiation. We envision that clinicians will value this NIR-triggerable system to help deliver the drug to solid tumors in a clinical application. Further in vivo studies are currently ongoing.

Received: January 9, 2013
Revised: February 21, 2013
Published online: March 12, 2013

Keywords: cancer · drug delivery · mesoporous materials · upconverting nanoparticles

[1] a) D. Peer, J. M. Karp, S. Hong, O. C. FaroKhzad, R. Margalit, R. Langer, *Nat. Nanotechnol.* **2007**, *2*, 751; b) T. M. Allen, P. R. Cullis, *Science* **2004**, *303*, 1818.

[2] a) J. E. Lee, N. Lee, T. Kim, J. Kim, T. Hyeon, *Acc. Chem. Res.* **2011**, *44*, 893; b) W. R. Zhao, J. L. Gu, L. X. Zhang, H. R. Chen, J. L. Shi, *J. Am. Chem. Soc.* **2005**, *127*, 8916; c) J. E. Lee, N. Lee, H. Kim, J. Kim, S. H. Choi, J. H. Kim, T. Kim, I. C. Song, S. P. Park, W. K. Moon, T. Hyeon, *J. Am. Chem. Soc.* **2010**, *132*, 552; d) Q. He, J. Shi, *J. Mater. Chem.* **2011**, *21*, 5845.

[3] a) Y. Zhu, M. Fujiwara, *Angew. Chem.* **2007**, *119*, 2291; *Angew. Chem. Int. Ed.* **2007**, *46*, 2241; b) J. Lu, E. Choi, F. Tamanoi, J. I. Zink, *Small* **2008**, *4*, 421; c) D. P. Ferris, Y.-L. Zhao, N. M. Khashab, H. A. Khatib, J. F. Stoddart, J. I. Zink, *J. Am. Chem. Soc.* **2009**, *131*, 1686; d) J. L. Vivero-Escoto, I. I. Slowing, C. W.

Wu, V. S. Y. Lin, *J. Am. Chem. Soc.* **2009**, *131*, 3462; e) S. Angelos, Y. W. Yang, N. M. Khashab, J. F. Stoddart, J. I. Zink, *J. Am. Chem. Soc.* **2009**, *131*, 11344; f) P. Yang, S. Gai, J. Lin, *Chem. Soc. Rev.* **2012**, *41*, 3679.

[4] K. Szaciłowski, W. Macyk, A. Drzewiecka-Matuszek, M. Brindell, G. Stochel, *Chem. Rev.* **2005**, *105*, 2647.

[5] a) M. Ochs, S. Carregal-Romero, J. Rejman, K. Braeckmans, S. C. De Smedt, W. J. Parak, *Angew. Chem.* **2013**, *125*, 723; *Angew. Chem. Int. Ed.* **2013**, *52*, 695; b) A. G. Skirtach, A. Muñoz Javier, O. Kreft, K. Köhler, A. Piera Alberola, H. Möhwald, W. J. Parak, G. B. Sukhorukov, *Angew. Chem.* **2006**, *118*, 4728; *Angew. Chem. Int. Ed.* **2006**, *45*, 4612.

[6] a) M. Haase, H. Schäfer, *Angew. Chem.* **2011**, *123*, 5928; *Angew. Chem. Int. Ed.* **2011**, *50*, 5808; b) Y. Yang, Q. Shao, R. Deng, C. Wang, X. Teng, K. Cheng, Z. Cheng, L. Huang, Z. Liu, X. Liu, B. Xing, *Angew. Chem.* **2012**, *124*, 3179; *Angew. Chem. Int. Ed.* **2012**, *51*, 3125; c) R. Deng, X. Xie, M. Vendrell, Y.-T. Chang, X. Liu, *J. Am. Chem. Soc.* **2011**, *133*, 20168; d) W. Wu, L. Yao, T. Yang, R. Yin, F. Li, Y. Yu, *J. Am. Chem. Soc.* **2011**, *133*, 15810; e) Y. Dai, P. a. Ma, Z. Cheng, X. Kang, X. Zhang, Z. Hou, C. Li, D. Yang, X. Zhai, J. Lin, *ACS Nano* **2012**, *6*, 3327; f) Y. Dai, D. Yang, P. a. Ma, X. Kang, X. Zhang, C. Li, Z. Hou, Z. Cheng, J. Lin, *Biomaterials* **2012**, *33*, 8704; g) S. Gai, P. Yang, C. Li, W. Wang, Y. Dai, N. Niu, J. Lin, *Adv. Funct. Mater.* **2010**, *20*, 1166; h) C. Li, J. Lin, *J. Mater. Chem.* **2010**, *20*, 6831; i) R. Kumar, M. Nyk, T. Y. Ohulchanskyy, C. A. Flask, P. N. Prasad, *Adv. Funct. Mater.* **2009**, *19*, 853; j) F. Vetrone, R. Naccache, V. Mahalingam, C. G. Morgan, J. A. Capobianco, *Adv. Funct. Mater.* **2009**, *19*, 2924; k) K. G. Jayakumar, N. M. Idris, Y. Zhang, *Proc. Natl. Acad. Sci. USA* **2012**, *109*, 8483; l) Q. Zhan, J. Qian, H. Liang, G. Somesfalean, D. Wang, S. He, Z. Zhang, S. Andersson-Engels, *ACS Nano* **2011**, *5*, 3744; m) Y. I. Park, H. M. Kim, J. H. Kim, K. C. Moon, B. Yoo, K. T. Lee, N. Lee, Y. Choi, W. Park, D. Ling, K. Na, W. K. Moon, S. H. Choi, H. S. Park, S.-Y. Yoon, Y. D. Suh, S. H. Lee, T. Hyeon, *Adv. Mater.* **2012**, *24*, 5755; n) C. Wang, H. Tao, L. Cheng, Z. Liu, *Biomaterials* **2011**, *32*, 6145.

[7] C. J. Carling, F. Nourmohammadian, J.-C. Boyer, N. R. Branda, *Angew. Chem.* **2010**, *122*, 3870; *Angew. Chem. Int. Ed.* **2010**, *49*, 3782.

[8] a) J.-C. Boyer, C.-J. Carling, B. D. Gates, N. R. Branda, *J. Am. Chem. Soc.* **2010**, *132*, 15766; b) C.-J. Carling, J.-C. Boyer, N. R. Branda, *J. Am. Chem. Soc.* **2009**, *131*, 10838.

[9] B. Yan, J.-C. Boyer, N. R. Branda, Y. Zhao, *J. Am. Chem. Soc.* **2011**, *133*, 19714.

[10] F. Chen, S. Zhang, W. Bu, Y. Chen, Q. Xiao, J. Liu, H. Xing, L. Zhou, W. Peng, J. Shi, *Chem. Eur. J.* **2012**, *18*, 7082.

[11] a) M. Lewin, N. Carlesso, C.-H. Tung, X.-W. Tang, D. Cory, D. T. Scadden, R. Weissleder, *Nat. Biotechnol.* **2000**, *18*, 410; b) H. Yuan, A. M. Fales, T. Vo-Dinh, *J. Am. Chem. Soc.* **2012**, *134*, 11358.

[12] N. Z. Knežević, B. G. Trewyn, V. S. Y. Lin, *Chem. Eur. J.* **2011**, *17*, 3338.

[13] a) J. Zhou, Y. Sun, X. X. Du, L. Q. Xiong, H. Hu, F. Y. Li, *Biomaterials* **2010**, *31*, 3287; b) H. Xing, W. Bu, Q. Ren, X. Zheng, M. Li, S. Zhang, H. Qu, Z. Wang, Y. Hua, K. Zhao, L. Zhou, W. Peng, J. Shi, *Biomaterials* **2012**, *33*, 5384.

[14] a) F. Wang, R. Deng, J. Wang, Q. Wang, Y. Han, H. Zhu, X. Chen, X. Liu, *Nat. Mater.* **2011**, *10*, 968; b) F. Chen, W. Bu, S. Zhang, X. Liu, J. Liu, H. Xing, Q. Xiao, L. Zhou, W. Peng, L. Wang, J. Shi, *Adv. Funct. Mater.* **2011**, *21*, 4285.

[15] N. Bogdan, F. Vetrone, G. A. Ozin, J. A. Capobianco, *Nano Lett.* **2011**, *11*, 835.

[16] a) L. Pan, Q. He, J. Liu, Y. Chen, M. Ma, L. Zhang, J. Shi, *J. Am. Chem. Soc.* **2012**, *134*, 5722; b) J. Kobler, K. Moller, T. Bein, *ACS Nano* **2008**, *2*, 791.

